Integrating towed streamer EM and 3D seismic data: from anisotropic resistivity to net-to-gross and total hydrocarbon volumes in place

Folke Engelmark, PGS*

Summary

The integration of Towed Streamer EM data with 3D seismic data offers unprecedented possibilities to extract quantitative estimates of the most important reservoir characteristics. The workflow is initiated using depth converted 3D seismic to build a sparse horizon model to constrain the inversion of towed streamer EM data. The total volume of the assumed reservoir is also estimated based on the seismic data. The EM inversion results yield, crucially, an estimate of anisotropy, here treated as simply the ratio of vertical (R_V) and horizontal (R_H) resistivity for the reservoir interval. By introducing estimated values for R_V and R_H of the shales that are inter-bedded with the reservoir sands, a range of net-to-gross (*N/G)* values can be defined that satisfies the inverted R_V and R_H for the entire reservoir. Based on pre-stack inverted seismic data, the *N/G* value can be further refined, and the porosity of the sands can also be estimated. With the improved knowledge of *N/G* together with the shale resistivity, it is possible to resolve the R_V and R_H for the sands, hence also including their effective anisotropy. The sand anisotropy arises as effective anisotropy when the hydrocarbon charged reservoir sands are layered in beds with different grain-sizes, resulting in hydrocarbon saturation and resistivity that increases with grain-size.
The final results offer estimates of the total reservoir volume, *N/G*, sandstone porosity, volumetric distribution of sand-beds by grain-size, each with their characteristic hydrocarbon saturation, and total hydrocarbon volumes in place.

Introduction

Controlled source EM (CSEM) methods have historically shown very qualitative results, typically with a transparent red blob over-plotted on a seismic section as background, indicating that a resistor exists somewhere within the colored blob. With the introduction of towed streamer EM offering acquisition efficiency similar to 2D seismic, real-time quality control, and much improved subsurface sampling density, new opportunities have opened up for joint EM and seismic solutions that are much more quantitative, as shown in Mattson et al (2013).

To get maximum value out of towed streamer EM data, and to facilitate extraction of quantitative information of value, EM has to be integrated with 3D seismic data. The workflow outlined here is shown as a proof of concept with reasonable values for all parameters that are introduced. The workflow also relies heavily on standard petrophysical models to estimate crucial parameters that are required to reach the goal of estimating the total hydrocarbon volumes in place.

The assumption in this proof of concept exercise is that the elastic properties of the reservoir and hydrocarbon fluids are such that the seismic data does not provide direct hydrocarbon indicators. Potential hydrocarbon charge has to be recognized as high resistivity by the EM data.
The seismic contribution starts with a depth converted sparse horizon model to constrain the EM inversion. The lateral boundaries of resistors are typically better constrained in the EM data than the depth of burial. Towed streamer EM detects resistors and the depth-converted pre-stack inverted data can confirm whether the resistor resides in a volume that has the appropriate range of elastic properties for a sandstone reservoir. Other resistors such as salt, basalt, granites, coal-beds and dense carbonates can be classified and dismissed as non-reservoir rocks. The pre-stack inverted seismic also contributes with crucial estimates of sandstone porosity and a calibration of *N/G* within the reservoir.

Workflow: proof of method

Depth converted 3D seismic data is used to build a sparse horizon-model to constrain the inversion of the EM data.

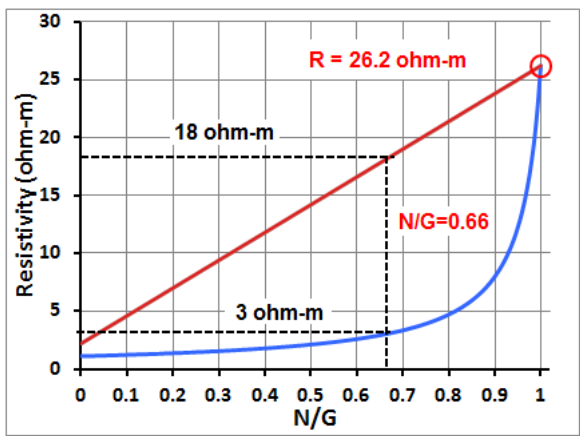

Figure 1: A graphic solution to find *N/G* and sand resistivity. The input data consists of R_H an R_V for the shales as 1.1 and 2.2 ohm-m respectively. The inverted R_H and R_V for the reservoir interval are 3.0 and 18.0 ohm-m respectively. The *N/G* trend-line for R_H (blue) is the harmonic average of the sand and shale resistivity, and the *N/G* trend-line for the R_V (red) is the arithmetic average of the sand and shale resistivity. The solutions for the *N/G* (0.66) and sand resistivity (26.2 ohm-m) are unique given the input data.

DOI http://dx.doi.org/10.1190/segam2014-0032.1

Towed streamer EM data can be inverted to vertical and horizontal resistivity indicating the anisotropy ratio for the target as well as the overburden. This is especially important for the evaluation of the assumed reservoir. The poor vertical resolution that is inherent in the diffusive nature of EM wave-propagation means the entire reservoir interval is typically represented by a single pair of vertical and horizontal resistivity values. The *N/G* and resistivity of the reservoir sands can be evaluated graphically as shown in Figure 1 above.

The cross-plot of *N/G* and resistivity has input data for the shales at *N/G* = 0.0 where the horizontal shale resistivity is 1.1 ohm-m, as measured by a deep induction log or estimated from seismic interval velocity as shown by Engelmark (2010). The trend-line for horizontal resistivity (blue line) as a function of *N/G* is calculated by taking the harmonic average of the horizontal shale resistivity and sand resistivity as a function of *N/G*. An estimated shale anisotropy of 2 renders the vertical shale resistivity as 2.2 ohm-m, and the trend-line for vertical resistivity (red line) is simply the arithmetic average of vertical shale and sand resistivity as a function of *N/G*. Further input data-points are the vertical resistivity at 18 ohm-m and the horizontal resistivity at 3 ohm-m from the inversion resulting in an anisotropy ratio of 6. It is easy to see that given the input data, the solutions for *N/G* (0.66) and sand resistivity (26.2 ohm-m) are unique if the sand is isotropic. Any other value for the sand resistivity results in two different values for the *N/G* where the 18 and 3 ohm-m lines intercept the trend-lines for vertical and horizontal resistivity.

Hydrocarbon charged reservoir sands can also exhibit anisotropy even if the porosity remains constant. In clean sands the irreducible water saturation, hence also the hydrocarbon saturation, is a function of grain-size, resulting in variations in resistivity. This gives rise to effective anisotropy when the individual beds cannot be resolved due to the poor vertical resolution that is the nature of diffusive EM wave-propagation. We can then expect a contribution to the overall anisotropy from inter-bedded sands displaying large-scale effective anisotropy. The upper limit of this contribution is when the reservoir is free from shale (*N/G* = 1) and all the observed anisotropy originates in the sands as shown in Figure 2 below.

The possible range in *N/G* is then a low of 0.66 for the case where the reservoir sands are effectively isotropic, to a maximum of 1.0, where the observed anisotropy originates entirely in the sands forming beds of different grain-sizes in a shale-free reservoir. This variation results in decreasing levels of irreducible water saturation ($S_{w\text{-}ir}$) with increasing grain-size. The hydrocarbon saturation (S_{hc}), or 1-$S_{w\text{-}ir}$, is then increasing with grain-size resulting in the resistivity also increasing with grain-size.

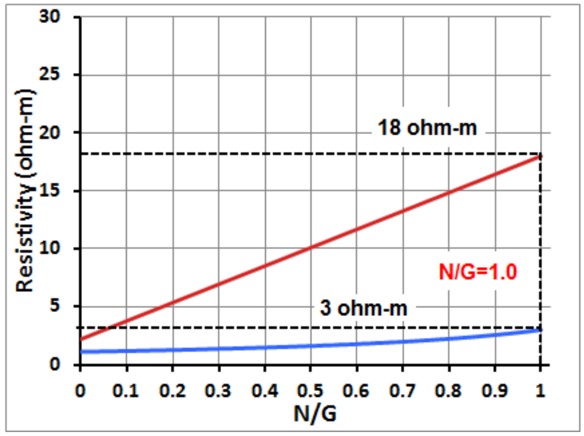

Figure 2: The upper limit of *N/G* is 1.0 indicating a shale-free reservoir. The observed anisotropy then originates as effective anisotropy due to inter-bedding of sands of different resistivity.

The fine-tuning of the *N/G* is performed with the aid of the seismic data. Pre-stack inverted 3D data is typically evaluated as a cross-plot between acoustic impedance (*AI*) and *Vp/Vs* as suggested in Figure 3.

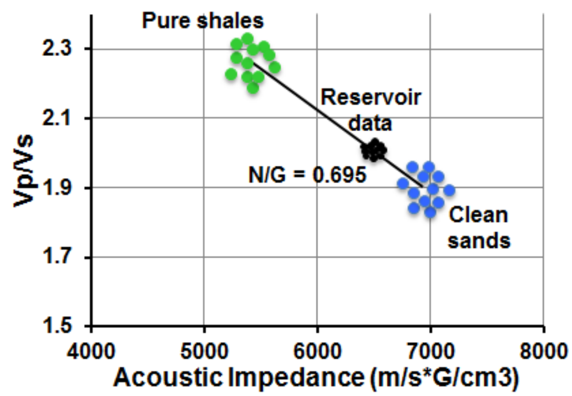

Figure 3: This cartoon illustrates how the *N/G* can be calibrated in a cross-plot of *AI* and *Vp/Vs* from the pre-stack inverted seismic data. The *N/G* is found to be 0.695.

The pure shales represent the *N/G* value of 0.0 whereas *N/G* is 1.0 for the clean sands. The *AI* may be lower, the same, or larger for the sands, but the *Vp/Vs* ratio is always larger for the shales. The *N/G* for the reservoir data is found by a linear interpolation between pure shales and clean sands. In this example the *N/G* is 0.695. A trend curve that describes the sand anisotropy as a function of *N/G* can be created by plotting the resulting *N/G* for a suite of sand anisotropy values between 0.0 and 6.0. The trend is specific to the shale anisotropy and overall reservoir anisotropy. In this example the sand anisotropy is found to be 2.0 for a *N/G* of 0.695 as seen in Figure 4. Porosity for the sands is evaluated to be 0.3 based on the AI information.

DOI http://dx.doi.org/10.1190/segam2014-0032.1

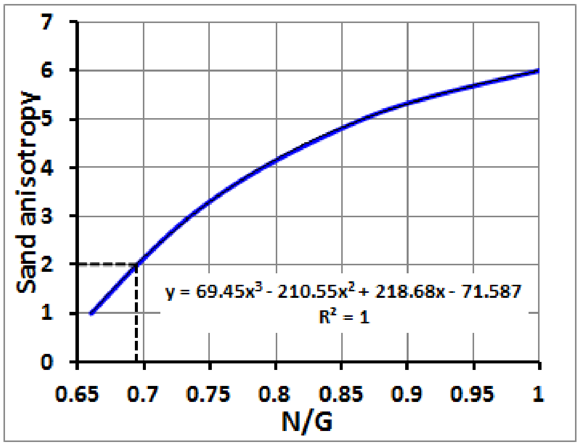

Figure 4: Given any particular shale and reservoir anisotropy a trend-line can be prepared for the relationship between *N/G* and sand anisotropy. The calibrated *N/G* of 0.695 corresponds to an effective sand anisotropy of 2.0 in this case.

A graphic solution to find the vertical and horizontal resistivity for the sands and the *N/G* for an effective sand anisotropy of 2.0 is seen in Figure 5.

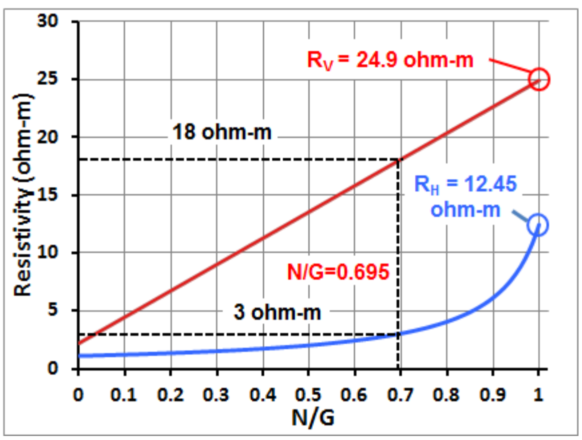

Figure 5: A graphic solution to find the R_V and R_H for the sands given the anisotropic resistivity of the shales, the effective anisotropy of the sands, and the *N/G* as input parameters.

As before the vertical and horizontal resistivities for the reservoir are 18.0 ohm-m and 3 ohm-m respectively. The shale resistivity remains unchanged and the effective vertical and horizontal resistivity for the sands are found to be 24.9 ohm-m and 12.45 ohm-m respectively for an anisotropy value of 2.0. The *N/G* is 0.695.

The next step involves modeling the resistivity of individual sands, all with a porosity of 0.3 but varying in grain size. Buckles (1965) was the first to observe that the product of irreducible water ($S_{w\text{-}ir}$) and porosity (ϕ) is constant for a clean well sorted sandstone of any particular grain size. The constants are known as Buckles numbers as seen in Table 1.

Grain-size (mm)	Buckle number	$S_{w\text{-}ir}$ (v/v)	R_t (ohm-m)
Very fine (1/16-1/8)	0.12	0.4	6.75
Fine (1/8 – 1/4)	0.06	0.2	27.0
Medium (1/4 – 1/2)	0.03	0.1	108
Coarse (1/2 – 1)	0.02	0.067	243

Table 1: The Buckle number is the product of $S_{w\text{-}ir}$ and ϕ. It is unique for each grain-size.

The calculation of the bulk rock resistivity (R_t) is based on the Archie (1942) equation:

$$R_t = \frac{a \cdot R_w}{\phi^m \cdot S_w^n} = \frac{0.81 \cdot 0.12}{0.3^2 \cdot S_w^2};$$

where a = tortuosity, R_w = resistivity of the pore water, m = cementation exponent, n = saturation exponent and S_w = water saturation = $S_{w\text{-}ir}$.

The values for a = 0.81; m = 2 and n = 2 were selected as typical values for a consolidated sandstone. The pore water was assumed to have a resistivity (R_w) of 0.12 ohm-m based on the assumption that at a nominal depth of burial of 1,500 m the salinity is 35,500 ppm and the formation temperature is 50 C.

The goal is to find a stack of sands where each bed has a different grain-size resulting in different resistivity. By varying the relative volumetric contribution of each sand-bed in the stack, the goal is to find the combination of sand-beds resulting in a vertical resistivity of 24.9 ohm-m by calculating the volumetrically weighted arithmetic average. At the same time the stack of sands also has to have a

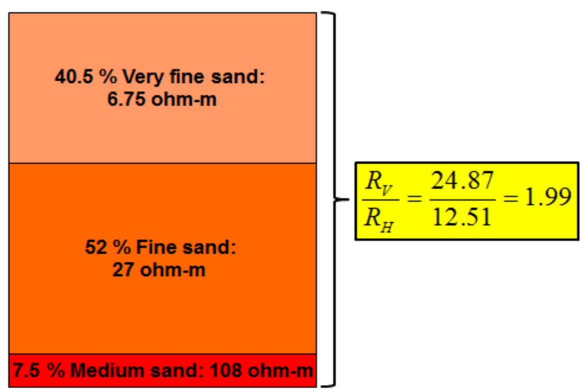

Figure 6: The reservoir sands exhibit an overall R_V = 24.9 ohm-m, a R_H = 12.45 ohm-m, hence an effective anisotropy of 2. The volumetric combination shown for the three sands in the model result in effective vertical and horizontal resistivity consistent with the effective anisotropy. Coarse sand is not part of the solution.

DOI http://dx.doi.org/10.1190/segam2014-0032.1

horizontal resistivity of 12.45 ohm-m when the volumetrically weighted harmonic average is calculated.

A solution that is consistent with what we know about the sands, namely the effective vertical and horizontal resistivity, is seen in Figure 6 above. Notice that coarse sand is not part of the solution. The minimum number of beds is shown in the figure, but they can be further split up into individual beds, as long as the total fractional volume of each grain-size is maintained. The order of beds is also immaterial. The *N/G* has also been estimated at 0.695, so the model for the entire reservoir has to consist of 69.5 % sand and 30.5 % shale.

Figure 7 shows a model that is consistent with what we know about the entire reservoir interval. The number of individual sand and shale beds can vary, as well as the order of the beds. However, the reservoir interval starts with a hydrocarbon charged sand at the top and ends with a charged sand at the bottom, and all three grain-sizes have to be present in the fractional volumes shown. The intra-bed shales have to be confined within the sand beds.

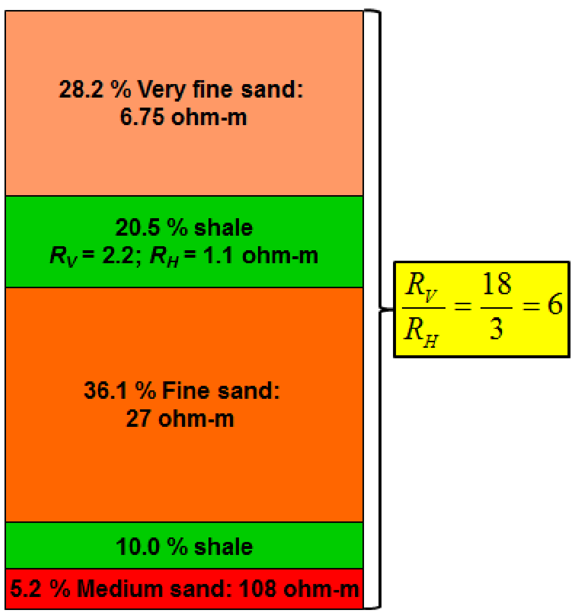

Figure 7: A final model for the reservoir drawn to scale: *N/G*: 0.695; R_V & R_H, at 18 and 3 ohm-m, respectively, are all consistent with the inverted EM data for the reservoir interval. The number of sand and shale beds can vary, but the total volumetric content of sand-beds sorted by grain-size, and the total shale volume (30.5 %) has to remain in agreement with the model.

The anisotropy for both sands and shales: 2; vertical shale resistivity: 2.2 ohm-m; horizontal shale resistivity 1.1 ohm-m; *N/G*: 0.695; vertical effective sand resistivity: 24.9 ohm-m; and horizontal effective sand resistivity: 12.45 ohm-m.

The sands make up 69.5 % of the reservoir and there are sand-beds of three grain-sizes: 28.2 % very fine sand; 36.1 % fine sand; and 5.2 % medium sand. There is no coarse sand present. The shales make up the remaining 30.5 %.

Table 2 shows the hydrocarbon contribution from each of the three grain-size classes of sand.

Sand fraction (v/v) by grain-size	$S_{w\text{-}ir}$ **(v/v)**	S_{hc} **(v/v)**	**Hydrocarbon volume**
Very fine (0.282)	0.4	0.6	0.05076
Fine (0.361)	0.2	0.8	0.08664
Medium (0.052)	0.1	0.9	0.01404

Table 2: The hydrocarbon volume for the sands, sorted by grain-size, is the product of sand fraction, hydrocarbon saturation, and porosity (0.3).

The hydrocarbon volume for the sands grouped by grain-size is the product of sand fraction, hydrocarbon saturation (S_{hc}) and porosity (0.3). The sum of the three (0.151) is the fraction of hydrocarbon within the total reservoir volume.

Conclusions

The workflow shown here, as a proof of concept, offers an unprecedented level of quantitative information extracted from an integrated solution facilitated by towed streamer EM and 3D seismic. The key contribution from EM is in the ability to estimate both vertical and horizontal resistivity for the reservoir interval. Together with estimated values for R_V and R_H for the inter-bedded shales, this provides sufficient information to determine a minimum *N/G* value for the case when the hydrocarbon-charged sands are effectively isotropic. The upper limit of *N/G* is 1.0 occurring when all the anisotropy originates in resistivity variations between sand-beds of different grain-size in a shale-free reservoir. The 3D seismic contributes with a sparse depth-converted horizon model to constrain the inversion of the EM data. Pre-stack inverted seismic contributes with an estimate of porosity for the reservoir sands and a calibration of the *N/G*, resolving the issue of how much the sands contribute to the overall effective anisotropy observed for the reservoir section. The final result is an estimate of *N/G* for the entire reservoir, and the volumetric fraction of sands of various grain-sizes, all with a characteristic hydrocarbon-saturation, leading to an estimate of the total hydrocarbon volumes in place. The total hydrocarbon volume originally in place that is consistent with all the data in this proof of concept example is found to be 15.1 % of the total reservoir volume.

Acknowledgements

The author would like to thank PGS for allowing the publication of this paper.

http://dx.doi.org/10.1190/segam2014-0032.1

EDITED REFERENCES

Note: This reference list is a copy-edited version of the reference list submitted by the author. Reference lists for the 2014 SEG Technical Program Expanded Abstracts have been copy edited so that references provided with the online metadata for each paper will achieve a high degree of linking to cited sources that appear on the Web.

REFERENCES

Archie, G. E., 1942, The electrical resistivity log as an aid in determining some reservoir characteristics: Transactions of AIME, 146, no. 1, 54–62, http://dx.doi.org/10.2118/942054-G.

Buckles, R. S., 1965, Correlating and averaging connate water saturation data: Journal of Canadian Petroleum Technology, **9**, no. 1, 42–52.

Engelmark, F., 2010, Velocity to resistivity transform via porosity: 80th Annual International Meeting, SEG, Expanded Abstracts, 2501–2505.

Mattsson, J., F. Engelmark, and C. Anderson, 2013, Towed streamer EM: The challenges of sensitivity and anisotropy: First Break, **31**, no. 6, 155–159.